

Kinetics and Mechanism for the Oxidation of CS₂ and COS at High Temperature

Yoshinori Murakami,* Masami Kosugi, Kenji Susa, Takaomi Kobayashi, and Nobuyuki Fujii

Department of Chemistry, Nagaoka University of Technology, Kamitomioka, Nagaoka 940-2188

(Received December 15, 2000)

The rate constants for the thermal decompositions of CS₂ and COS were investigated by measuring the time profiles of S atom using atomic resonance absorption spectroscopy behind the incident shock of CS₂/Ar or COS/Ar mixtures, and the rate constants were determined to be $k = (4.0 \pm 0.1) \times 10^{14} \exp(-295 \pm 20 \text{ kJ}/RT) \text{ cm}^3 \text{ mol}^{-1} \text{ s}^{-1}$, T : 2200–2900 K and $k = (1.4 \pm 0.3) \times 10^{15} \exp(-290 \pm 25 \text{ kJ}/RT) \text{ cm}^3 \text{ mol}^{-1} \text{ s}^{-1}$, T : 2000–3200 K, respectively. The oxidation mechanism of COS was also investigated behind the incident shock of COS/O₂/Ar mixtures and the rate constant for the reaction $\text{S} + \text{O}_2 \rightarrow \text{SO} + \text{O}$ was obtained to be $k = (9.5 \pm 0.7) \times 10^{13} \exp(-41 \pm 28 \text{ kJ}/RT) \text{ cm}^3 \text{ mol}^{-1} \text{ s}^{-1}$, T : 2200–2900 K. From a numerical analysis for time profiles of S atom behind the incident shock of CS₂/O₂/Ar mixtures, the rate constant for the reaction $\text{O} + \text{CS} \rightarrow \text{CO} + \text{S}$ was expressed as $k = (3.2 \pm 1.0) \times 10^{13} \text{ cm}^3 \text{ mol}^{-1} \text{ s}^{-1}$, T : 2100–3000 K. Similarly, the rate constant for the reaction $\text{CS} + \text{O}_2 \rightarrow \text{COS} + \text{O}$ was also determined to be $k = (6.1 \pm 0.6) \times 10^{12} \exp(-51.0 \pm 68 \text{ kJ}/RT) \text{ cm}^3 \text{ mol}^{-1} \text{ s}^{-1}$, T : 2000–2900 K by measuring the time profiles of O atom behind the reflected shock of CS₂/O₂/Ar mixtures. Ab initio calculations were carried out and the reaction pathways of $\text{CS} + \text{O}_2 \rightarrow \text{COS} + \text{O}$ and $\text{CS} + \text{O}_2 \rightarrow \text{CO} + \text{SO}$ were also investigated.

Carbon disulfide is known to be an important sulfur-containing species, and understanding the mechanism for the oxidation of carbon disulfide is also important for understanding such environmental problems as acid rain. Since the 1930's, several researchers have tried to determine the explosion limits of CS₂ oxidation as a function of temperature, and have discussed the explosion limits based on the kinetic model of CS₂ oxidation.^{1,2} To explain the explosion limits of CS₂/O₂ mixtures, Wood and Heicklen³ proposed the importance of the following branching chain reaction:



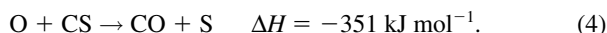
and subsequent reactions of CS with O₂ molecule:



On the other hand, some researchers^{4,5} concluded that CS radical didn't play important roles in the oxidation mechanism of CS₂, and that CS radical was lost at the wall of the reactor during the oxidation of CS₂ because of the low reactivity of CS radical with O₂ molecule. A recent kinetic study of $\text{CS} + \text{O}_2$ reaction suggested that the overall rate constant of this reaction is very slow (i.e. $k = 1.7 \times 10^5 \text{ cm}^3 \text{ mol}^{-1} \text{ s}^{-1}$) at room temperature.⁶ Richardson⁷ measured the rate constant for this reaction under the temperature range between 290–500 K using a discharge flow tube with a mass spectrometer. However, the rate constant for this reaction has not been measured at temperatures higher than 500 K.

The other possible pathway of CS removal is the $\text{O} + \text{CS}$

reaction. This reaction is known to produce highly vibrationally excited CO molecules via



The vibrational distribution of CO produced by this reaction was investigated by several researchers,^{8,9} the results of which showed that CO was populated even up to high vibrational levels ($v = 15$). Therefore, such a population inversion of CO was applied for chemical-pumped CO lasers.¹⁰ On the other hand, the rate constant for the reaction $\text{O} + \text{CS} \rightarrow \text{CO} + \text{S}$ was first investigated by Slage et al.¹¹ They determined the rate constant for this reaction to be $k = 1.24 \times 10^{13} \text{ cm}^3 \text{ mol}^{-1} \text{ s}^{-1}$ using a flow-tube technique with photoionization mass spectrometry. Bida et al.¹² also measured the rate constant by monitoring the decay of CS by a multipath absorption technique at 257.6 nm. They concluded that the reaction $\text{O} + \text{CS} \rightarrow \text{CO} + \text{S}$ is very rapid and that the obtained rate constant is in good agreement with that obtained by Slage et al. The temperature dependence of the reaction rate was measured by Lienfeld and Richardson¹³ using a fast-flow reactor with an electron-spin resonance mass spectrometer, but the temperature range was below 300 K, which was far below the flame temperature.

Similar to the case of CS₂ oxidation, the oxidation of COS is known to play the important roles in the combustion of sulfur-containing compounds. Above 2000 K, the initial process of COS oxidation is considered in the following reaction scheme:



Pioneering work on determining the rate constant for the thermal decomposition of COS was carried out by Schecker and Wagner.¹⁴ Recently, Woiki and Roth¹⁵ measured this rate constant; their result was found to be in good agreement with each other. Oya et al.¹⁶ also measured the rate constant, and it was also confirmed that the rate constant for reaction (5) was similar to the results obtained by previous researchers. On the other hand, measurements of the rate constant for reaction (6) at high temperature have been limited until recently. Saito et al.¹⁷ measured the rate constant by monitoring the O-atom production in COS/O₂/Ar mixtures for the first time at a temperature range higher than 1000 K. Later, Miyoshi et al.¹⁸ and Woiki and Roth¹⁹ re-investigated the rate constant for reaction (6) by monitoring S atoms behind the reflected shock waves of COS/O₂/Ar mixtures or after 248-nm photolysis of COS/O₂/Ar mixtures behind the reflected shock waves.

For kinetic measurements of combustion phenomena, using a shock-tube is convenient method to measure the rate constants for elementary reactions relevant to the combustion processes because of the uniform temperature profile and no disturbance from heterogeneous reactions at the wall of the reactor. Especially, atomic resonance absorption spectrometry (ARAS), which monitors the time profiles of the absorption of atomic species, like H and O during high-temperature reactions, is successfully used to determine the rate constants of elementary reactions behind the shock waves at temperatures higher than 1000 K.²⁰ Although the shock-tube apparatus was already applied to study the oxidation mechanism of carbon disulfide by Sheen et al.,²¹ no kinetic investigations on the time profiles of atomic species were carried out using the shock-tube apparatus. Since S and O-atoms are important carriers of chain reactions, the temporal behaviors of these species are of particular importance for understanding the combustion of CS₂/O₂ mixtures. In the present work, the time profiles of S and O-atoms were monitored using ARAS techniques behind the incident or reflected shock of CS₂/O₂/Ar mixtures. By kinetic simulations of these temporal profiles of atomic species, the rate constants for the reactions O + CS → CO + S and CS + O₂ → COS + O were mainly determined above 2000 K. The oxidation mechanism of COS was also investigated by monitoring S atoms behind the incident shock of COS/Ar and COS/O₂/Ar mixtures and the rate constants for the reactions (5) and (6) were determined. All of these higher-temperature results were compared with previous works; further, the fate of CS₂ and COS at the flame temperature was discussed.

Experimental

A schematic of the experimental apparatus is shown in Fig. 1. The shock-tube apparatus is a conventional diaphragm shock-tube of 46 mm internal diameter and 3.6 m long at the low-pressure section. Shock was driven with high-pressure hydrogen or helium gas, and before each run the driven section was pumped down to pressures below 5×10^{-5} Torr by a diffusion pump. The temperature and pressure behind the shock waves were calculated from the incident shock velocities. The incident shock velocities were measured by four piezoelectric transducers, and the mean shock velocity was used for a calculation.

The shock tube was equipped with atomic resonance absorption spectroscopy diagnostics consisting of a microwave discharge

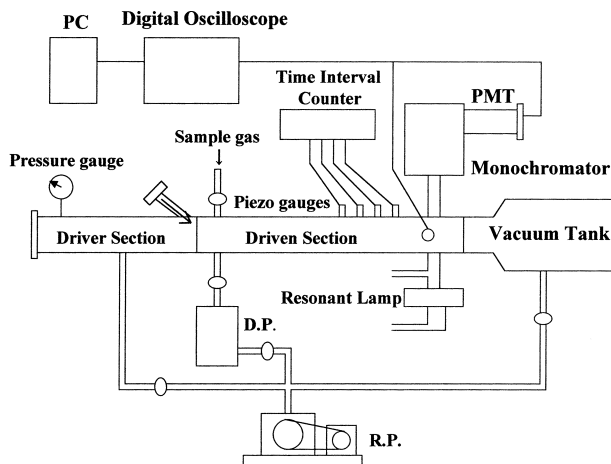


Fig. 1. Schematic figure of experimental setup.

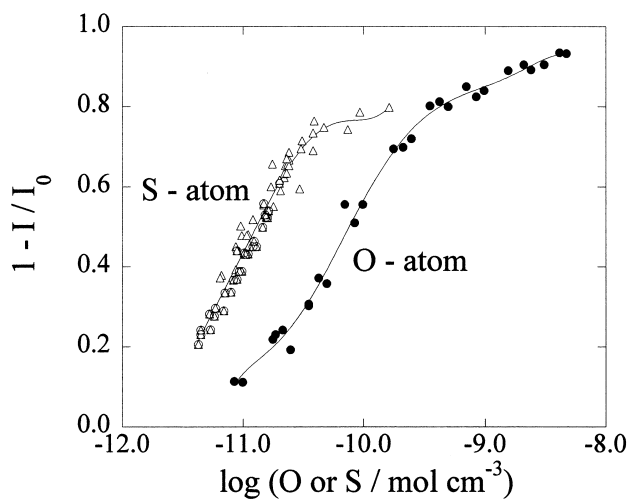


Fig. 2. Relationship between O- and S-ARAS signal intensities and their concentrations.

lamp, a vacuum-UV monochromator (Ritsu MCV-20) and a solar-blind photo-multiplier (Hamamatsu R-1080). The gases for the light sources for the absorption measurements of O and S atoms were 1% O₂ and 0.1% H₂S diluted in helium, respectively. Each time profile of the atomic absorption signal obtained in the solar-blind photo-multiplier was stored in an oscilloscope (Tektronix 2201) and sent to a personal computer for further analysis.

Each absorption signal was calibrated to obtain the relationship between the signal intensities and the concentrations. In the case of the calibration of O atoms at 130.5 nm, the thermal decomposition of N₂O was used. By varying the concentration of N₂O/Ar mixtures, the relationship between the O-atom concentration and $1 - I/I_0$ was determined. The relationship between the O-atom concentration and $1 - I/I_0$ is shown in Fig. 2. Here, I and I_0 are the transmitted and incident lights of a microwave discharge lamp, respectively. Similarly, a calibration of S atom at $\lambda = 182.6$ nm was performed using CS₂/Ar and COS/Ar mixtures. Since all of CS₂ and COS thermally decompose to produce S atoms, the relationship between the signal intensities and S-atom concentrations can be determined by calculating the initial concentrations of CS₂ or COS behind the shock waves. The results are also shown in

Table 1. Reaction Scheme and Rate Constants^{a)} in the CS₂/O₂/Ar Mixtures

Reaction	A		Reference
	$\text{cm}^3 \text{mol}^{-1} \text{s}^{-1}$	E_a kJ	
O + CS ₂ = CS + SO	3.6×10^{13}	7.1	31
OS + O ₂ = O + COS	6.1×10^{12}	51	this work
O + CS = CO + S	3.2×10^{13}	0.0	this work
COS + Ar = CO + S + Ar	1.4×10^{15}	290	this work
S + O ₂ = SO + O	9.5×10^{13}	41	this work
CS ₂ + Ar = CS + S + Ar	4.0×10^{14}	290	this work
O + CS ₂ = CO + S ₂	1.7×10^{12}	5.0	11
O + CS ₂ = COS + S	7.1×10^{12}	8.8	11
S + CS ₂ = CS + S ₂	1.0×10^{14}	17	30
SO + O ₂ = SO ₂ + O	4.5×10^{11}	27	31
COS + O = CO + SO	1.6×10^{13}	19	31
S ₂ + O = SO + S	4.0×10^{12}	0	32
COS + O = CO ₂ + S	1.2×10^{14}	46	32
CS ₂ + O ₂ = CS + SO ₂	1.0×10^{12}	130	33

a) Rate constants in the form, $k = A \exp(-E_a/RT)$ in cm, mol, kJ and K units.

Fig. 2. As shown in Fig. 2, no pressure and temperature dependences of these calibration curves were observed. In the present work, all experiments were performed at $1 - III_0 < 0.5$ because a higher $1 - III_0$ didn't give a linear relationship between $1 - III_0$ and the atomic concentrations.

For simulating the temporal profiles of atomic species behind the incident or reflected shock by numerical calculations, we used the Chemkin²² and Chemkin thermodynamic database.²³ The kinetic schemes used in the present work are shown in Table 1. The program can also calculate the rate constant for the backward reaction for each reaction given in Table 1 through the equilibrium constant using the thermodynamic functions of the species involved.

CS₂ (99%; Nacalai tesque) and COS (97.5%; Matheson) used in this work were purified by trap-to-trap distillation using dry ice and liquid N₂. Ar (99.9995%; Taiyo Sanso) and O₂ (99.995%; Taiyo Sanso) were used without further purification.

Results and Discussion

1 Thermal Decomposition of CS₂ and COS. Several researchers have already investigated the rate constant for the thermal decomposition of CS₂. We also tried to determine the rate constant for the reaction $\text{CS}_2 + \text{Ar} \rightarrow \text{CS} + \text{S} + \text{Ar}$ by measuring the time profiles of S atoms behind the incident shock of CS₂/Ar mixtures. Figure 3 is a typical example of S-atom time profiles. Here, the time axis is converted to the real gas time. As shown in the figure, S atoms produced rapidly behind the incident shock, reaching an equilibrium value after 700 μs , where CS₂ decomposed completely at temperatures higher than about 2500 K. Since the initial concentration of CS₂ diluted in Ar was as low as few ppm, the subsequent reaction, $\text{S} + \text{CS}_2 \rightarrow \text{CS} + \text{S}_2$, had a negligible contribution on the time profile of S atoms. A comparison of the kinetic calculation with the experimental profile is shown in Fig. 3, and the calculated profiles using the k_1 values doubled and halved are also shown in the figure. From these calculated lines, the accuracy of the values is shown to be high. The resultant Arrhenius form of the rate constants obtained for the reaction $\text{CS}_2 + \text{Ar} \rightarrow \text{CS} + \text{S} + \text{Ar}$ is shown in Fig. 4. As shown in this figure,

the rate constant for the reaction was determined to be $k_7 = (4.0 \pm 0.1) \times 10^{14} \exp(-290 \pm 20 \text{ kJ}/RT) \text{ cm}^3 \text{ mol}^{-1} \text{ s}^{-1}$ in the temperature range of 2200 to 2900 K, and was in good agreement with those obtained by Gaydon et al.²⁴ and by Olschewski et al.,²⁵ but about three-times larger than the value obtained by Saito et al.²⁶

The rate constant for the thermal decomposition of COS was also investigated by measuring the time profiles of S atoms behind the incident shock of COS/Ar mixtures. Figure 5 shows an example of the S-atom time profile. Based on a kinetic calculation it was confirmed that S atoms were solely

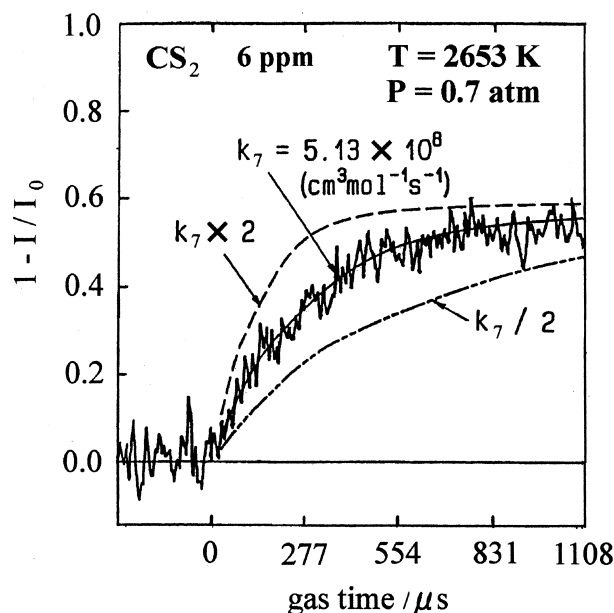


Fig. 3. Typical absorption profile at 182.6 nm for CS₂/Ar system.

Conditions: $T = 2653 \text{ K}$, $P = 0.7 \text{ atm}$, $\text{CS}_2 = 6 \text{ ppm}$.

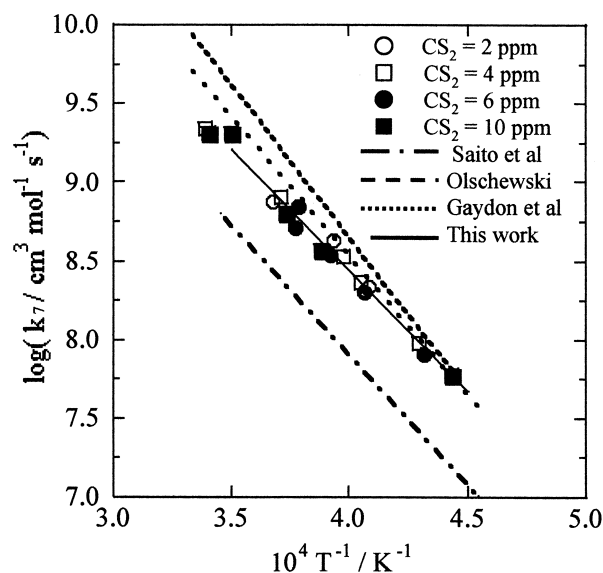


Fig. 4. Arrhenius plot of measured second-order rate constant for $\text{CS}_2 + \text{Ar} \rightarrow \text{CS} + \text{S} + \text{Ar}$.

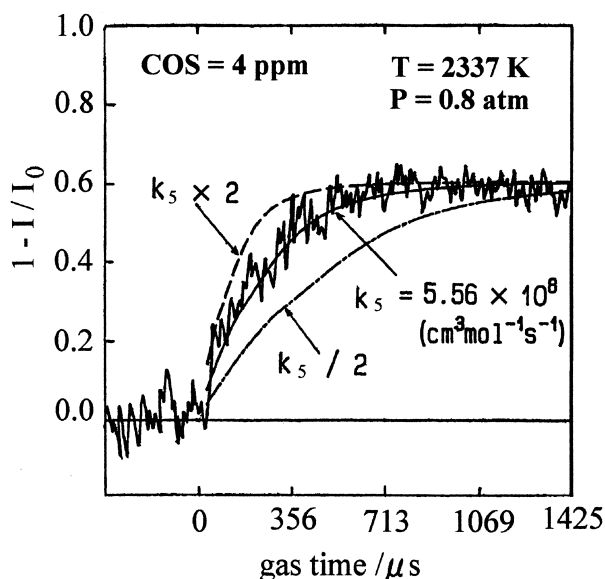


Fig. 5. Typical absorption profile at 182.6 nm for COS/Ar system.

Conditions: $T = 2337$ K, $P = 0.8$ atm, COS = 4 ppm.

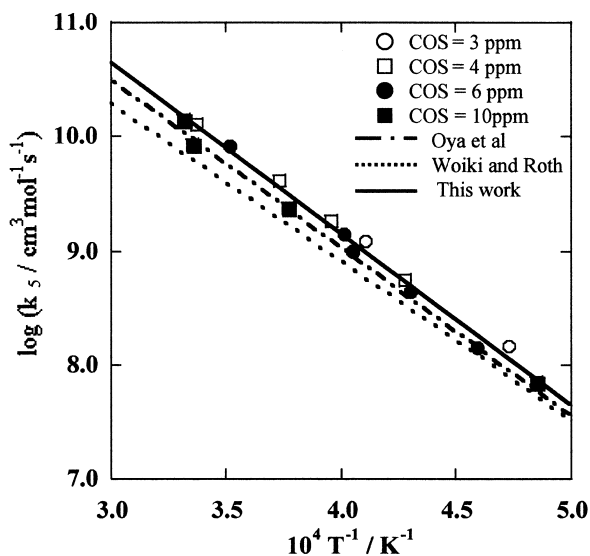


Fig. 6. Arrhenius plot of measured second-order rate constant for COS + Ar \rightarrow CO + S + Ar.

produced by the thermal decomposition, COS + Ar \rightarrow CO + S + Ar, and that a subsequent reaction, such as S + COS \rightarrow CO + S₂, had negligible contributions on the time profiles of S atoms under our experimental conditions. The Arrhenius form of the rate constant is shown in Fig. 6, and the rate constant was determined to be $k_5 = (1.4 \pm 0.3) \times 10^{15} \exp(-290 \pm 25 \text{ kJ}/RT) \text{ cm}^3 \text{ mol}^{-1} \text{ s}^{-1}$ in the temperature range of 2000 to 3200 K. The Arrhenius forms of the rate constant for this reaction obtained by previous workers are also shown in Fig. 6. As shown in Fig. 6, the present results are in good agreement with previous works using the S-ARAS technique by Woiki et al.¹⁵ and Oya et al.¹⁶

2 High-Temperature Oxidation of COS. Time profiles of S atoms behind the incident shock of COS/O₂/Ar mixtures

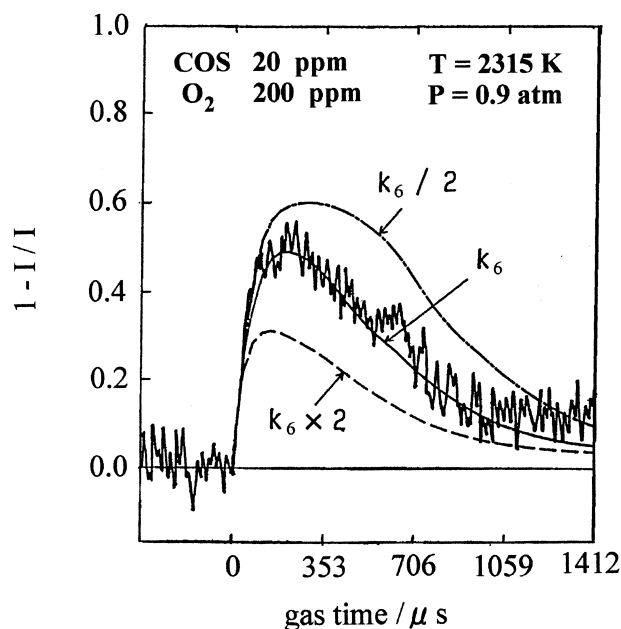


Fig. 7. Typical absorption profile at 182.6 nm for COS/O₂/Ar system.

Conditions: $T = 2315$ K, $P = 0.9$ atm, COS = 20 ppm, O₂ = 200 ppm.

are shown in Fig. 7. As shown in Fig. 7, S-atom formation followed by fast decay was observed. Because the decay of S atoms is only responsible for the reaction S + O₂ \rightarrow SO + O, the rate constant for this reaction can be determined by simulating the decay of the time profile of S atoms behind the incident shock of COS/O₂/Ar mixtures using all of the reactions tabulated in Table 1. A sensitivity analysis using the reaction schemes shown in Table 1 was performed, and it was confirmed that only reactions (5) and (6) were responsible to the time profile of S atom. Therefore, the other reactions had little influence on the determination of the rate constant for reaction (6). The rate constant obtained in this work was $k_6 = (9.5 \pm 0.7) \times 10^{13} \exp(-41 \pm 28 \text{ kJ}/RT) \text{ cm}^3 \text{ mol}^{-1} \text{ s}^{-1}$ between $T = 2200$ and 2900 K, and the present rate expression compared to previous ones is plotted in Fig. 8. As can be seen in the figure, the rate constant obtained in this work is much higher than that obtained by Saito et al.¹⁷ In addition, a slight curvature of the Arrhenius forms of the rate constant was observed, combined with previous works by Miyoshi et al.¹⁸ and Woiki and Roth.¹⁹

3 High-Temperature Oxidation of CS₂. A typical example of the time profiles of S atoms behind the incident shock of CS₂/O₂/Ar mixtures is shown in Fig. 9. The time profile of S atom in the figure showed a fast increase at an early reaction time, followed by a slow decay compared with the case of COS oxidation. To simulate the time profiles of S atom obtained in this work, numerical simulations were performed using the reaction scheme in Table 1. The results are also shown by line (a) in Fig. 9. It can be seen that the agreement between the experiment and computation is not good. To find the reason for such a disagreement, a sensitivity analysis of the time profiles of S atom on the rate constants for reactions were carried out under the same experimental conditions as in Fig. 9. Here, the sensitivity is expressed as $(d[S]/dk) (k/[S])$, where $(k/$

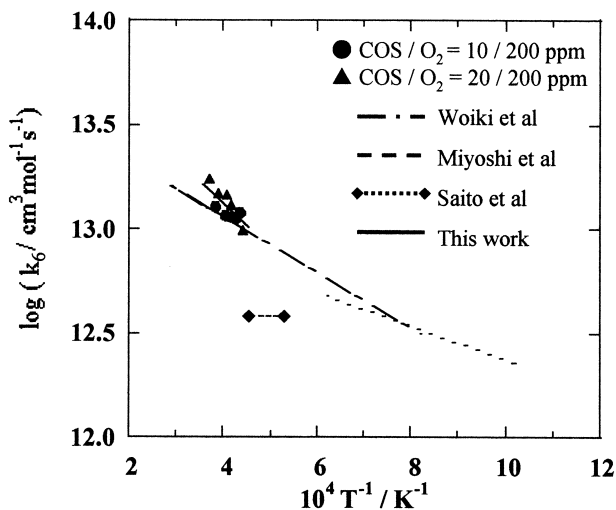


Fig. 8. Arrhenius plot of measured rate constant for $S + O_2 \rightarrow SO + O$.

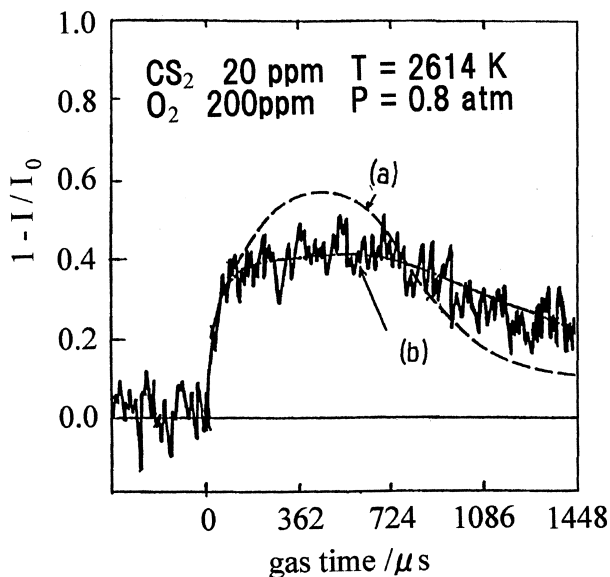


Fig. 9. Typical absorption profile at 182.6 nm for $CS_2/O_2/Ar$ system.

Conditions: $T = 2614$ K, $P = 0.8$ atm, $CS_2 = 20$ ppm, $O_2 = 200$ ppm.

$[S]$) is used to normalize the $(d[S]/dk)$ values. The results are shown in Fig. 10. From a sensitivity analysis the following reactions:



were found to be sensitive to the slow-decay part of the S atom profiles, and the other reactions were less sensitive to that of S atom compared to the above three reactions.

Since the rate constants for reactions (7) and (6) have al-

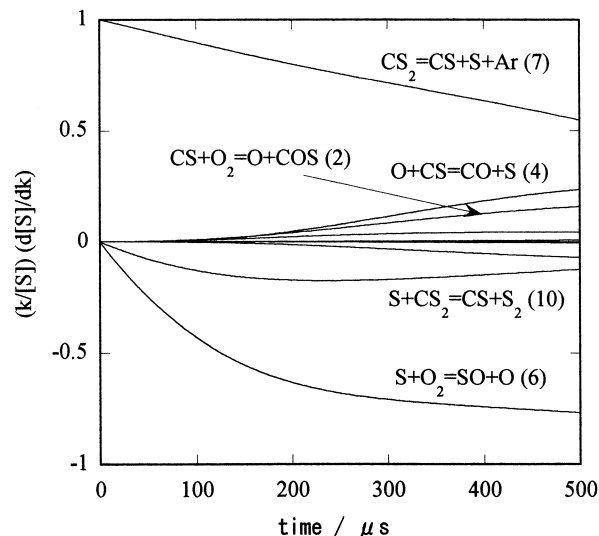


Fig. 10. Sensitivity analysis of time profile of S atom in the CS_2/O_2 reaction system.

Conditions: $T = 2614$ K, $P = 0.8$ atm, $CS_2 = 20$ ppm, $O_2 = 200$ ppm.

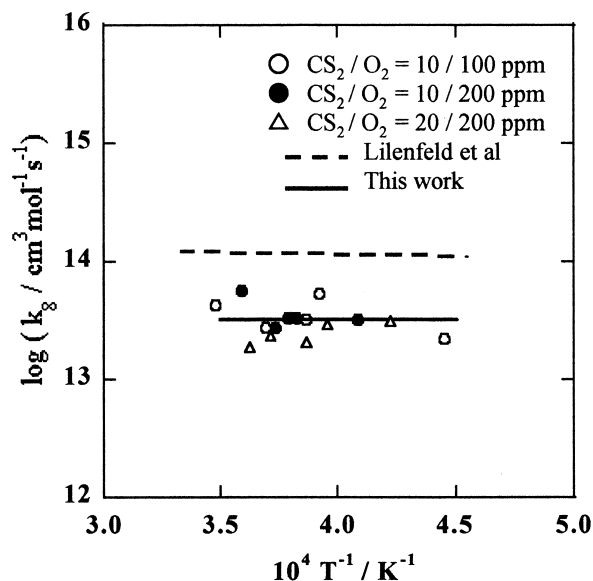


Fig. 11. Arrhenius plot of measured rate constant for $O + CS \rightarrow CO + S$.

ready obtained in this work, we can determine the rate constant for reaction (4). Although the rate constant for reaction (4) was determined previously by Slage et al.¹¹ and by Bida et al.¹² below 300 K, it is doubtful that the rate constant for reaction (4) is correct, even under our high-temperature experimental conditions. Therefore, the rate constant for reaction (4) was re-investigated by simulating the time profiles of S atom obtained behind the incident shock of $CS_2/O_2/Ar$ mixtures. Line (b) in Fig. 9 shows the simulated profile using the rate constant for reaction (4) obtained by fitting work. The best fit to our experimental profiles gave the rate constant $k_4 = (3.2 \pm 1.0) \times 10^{13} \text{ cm}^3 \text{ mol}^{-1} \text{ s}^{-1}$ for reaction (4) in the temperature range of $T = 2100$ to 3000 K. Figure 11 shows Arrhenius plots of the

rate constant for the reaction $\text{O} + \text{CS} \rightarrow \text{CO} + \text{S}$. Compared to the results obtained by Lienfeld et al. below 300 K,¹³ our result was about one third of their rate constant. Also, the activation energy for the reaction was found to be small, which is the same conclusion as that by Lienfeld et al.

The time profiles of the O atom in the CS₂/O₂/Ar reaction system were also measured using the atomic resonance absorption spectrometry technique. Because of a modification of the experimental apparatus, the measurement was carried out behind the reflected shock of CS₂/O₂/Ar mixtures, and diaphragm-

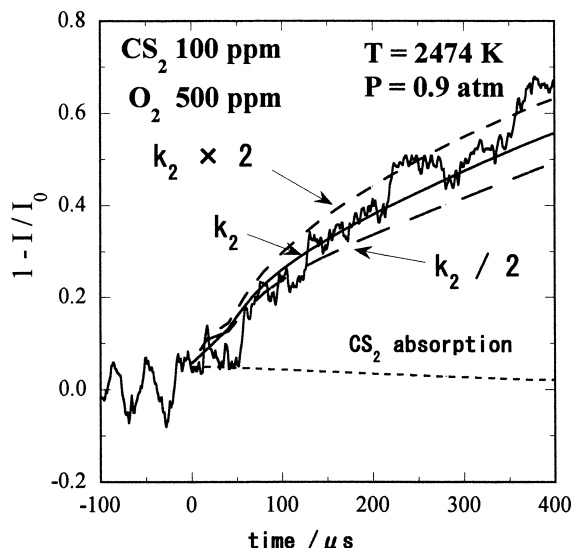


Fig. 12. Typical absorption profile at 130.5 nm for CS₂/O₂/Ar system.

Conditions: $T = 2474 \text{ K}$, $P = 0.9 \text{ atm}$, $\text{CS}_2 = 100 \text{ ppm}$, $\text{O}_2 = 500 \text{ ppm}$.

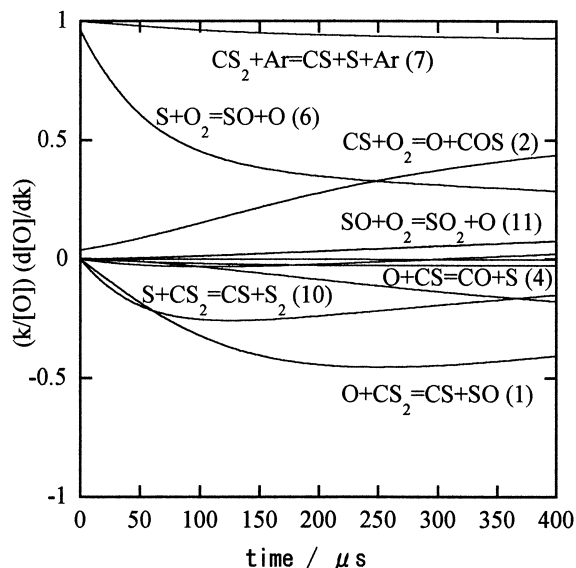


Fig. 13. Sensitivity analysis of time profile of O atom in the CS₂/O₂ reaction system.

Conditions: $T = 2474 \text{ K}$, $P = 0.9 \text{ atm}$, $\text{CS}_2 = 100 \text{ ppm}$, $\text{O}_2 = 500 \text{ ppm}$.

less shock-tube was used instead of the conventional diaphragm shock-tube. A typical example of the time profile of O atom is shown in Fig. 12. Because of some absorption of CS₂ at 130.5 nm, a certain amount of absorption was observed just behind the reflected shock wave at the $t = 0$ position. Hence, such molecular absorption of CS₂ at 130.5 nm was included in the kinetic simulations by using the absorption coefficient measured by Hatarajan and Roth.²⁷ Other molecular absorption was found to be of little influence on the time profiles of O atom. Similar to the case of S-ARAS in the CS₂/O₂/Ar system, a sensitivity analysis of the O-atom time profiles in the CS₂/O₂/Ar system were performed using the reaction scheme shown in Table 1. As shown in Fig. 13, the reactions $\text{O} + \text{CS}_2 \rightarrow \text{CS} + \text{SO}$ and $\text{CS} + \text{O}_2 \rightarrow \text{COS} + \text{O}$ as well as the reactions $\text{CS}_2 + \text{Ar} \rightarrow \text{CS} + \text{S} + \text{Ar}$ and $\text{S} + \text{O}_2 \rightarrow \text{SO} + \text{O}$ were sensitive to the time profile of O atom compared to the other reactions. Since the rate constant for the reaction $\text{O} + \text{CS}_2 \rightarrow \text{CS} + \text{SO}$ has already been investigated by several researchers^{11,28-31} using discharge-flow techniques, and their results are almost in good agreement with each other, we used the recommended value of this rate constant derived from their experimental results, and tried to determine the rate constant for the reaction $\text{CS} + \text{O}_2 \rightarrow \text{COS} + \text{O}$ by simulating the O-atom time profiles in the CS₂/O₂/Ar system. In these kinetic simulations of O atom, the present results were used for the rate constants for the reactions $\text{CS}_2 + \text{Ar} \rightarrow \text{CS} + \text{S} + \text{Ar}$ and $\text{S} + \text{O}_2 \rightarrow \text{SO} + \text{O}$. By a slight modification of the rate constant for the reaction $\text{CS} + \text{O}_2 \rightarrow \text{COS} + \text{O}$ tabulated in Table 1, agreements between the experimental profiles and kinetic simulations were obtained. The results of kinetic simulations using Table 1 are also shown in Fig. 12. Figure 14 shows the Arrhenius plots of the rate constant of the reaction $\text{CS} + \text{O}_2 \rightarrow \text{O} + \text{COS}$. A least-squares fit of the rate constants lead to the following Arrhenius expression: $k_2 = (6.1 \pm 0.6) \times 10^{12} \exp(-51.0 \pm 68 \text{ kJ/RT}) \text{ cm}^3 \text{ mol}^{-1} \text{ s}^{-1}$ in the temperature range of 2000 to 2900 K. As shown in Fig. 14, the rate constant obtained in this work is almost similar to a previous estimate by Howgate et al.³²

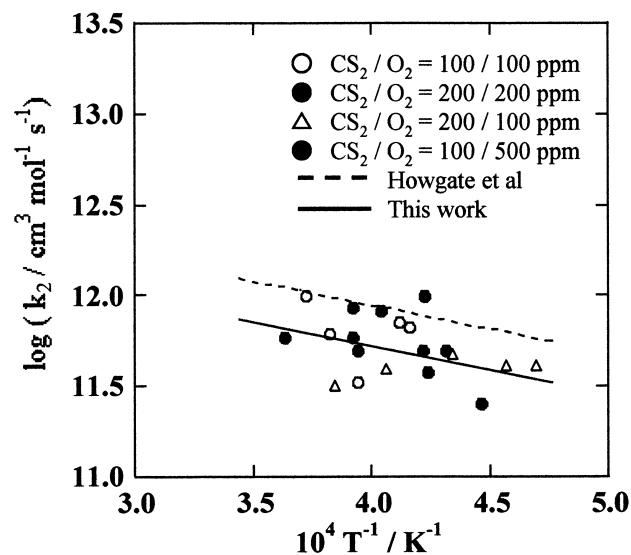


Fig. 14. Arrhenius plot of measured rate constant for $\text{CS} + \text{O}_2 \rightarrow \text{COS} + \text{O}$.

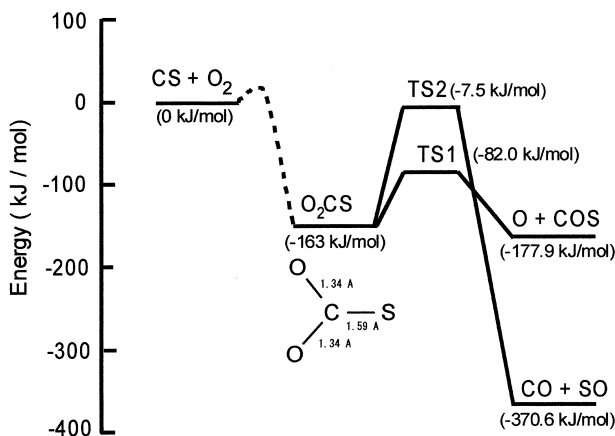


Fig. 15. Energy diagram for reaction of CS + O₂ at the level of MP2/6-31G(d) theory.

The reaction of CS with O₂ molecule is considered to have the following two reaction channels,



In this work we assumed that the rate constant for the latter reaction (3) had negligible contributions compared with the former reaction (2), as proposed by Sheen et al.²¹ To make sure that this assumption was correct, ab-initio calculations at the level of UMP2(full)/6-31G(d)//UMP2(full)/6-31G(d) were performed to find the pathways of the CS + O₂ reaction. All calculations were performed by Gaussian98.³³ The energy diagram for the CS + O₂ reaction is shown in Fig. 15. Although the level of calculations is not sufficiently high, a quantitative picture of the reaction pathways is usefully described in this energy diagram. As shown in the energy diagram, the first step of the CS + O₂ reaction is the formation of an adduct, CSO₂. The planar adduct CSO₂ has two pathways. One is cleavage of the CO bond to form COS and O (see TS1); the other is to go through the triangular transition state TS2 to form CO and SO. The structures and vibrational frequencies of the transition states (TS1 and TS2) are shown in Fig. 16 and Table 2, respectively.

According to RRKM theory, the microcanonical rate constant is expressed as $k(E^*) = G(E^+)/h \times N(E^*)$. Here $N(E^*)$

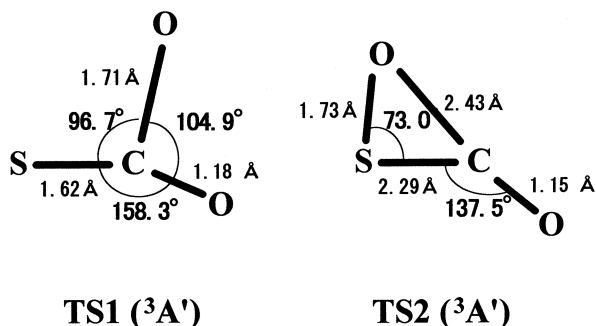


Fig. 16. Calculated structures of transition states at UMP2(full)/6-31G(d) level of theory.

Table 2. Vibrational Frequencies of Transition States Calculated at the Level of UHF/6-31G(d)

Transition states	Vibrational frequencies ^{a)} /cm ⁻¹					
TS1	1294i,	263,	341,	544,	639,	1922
TS2	308i,	169,	197,	390,	736,	2022

a) Vibrational frequencies scaled with 0.893 are given.

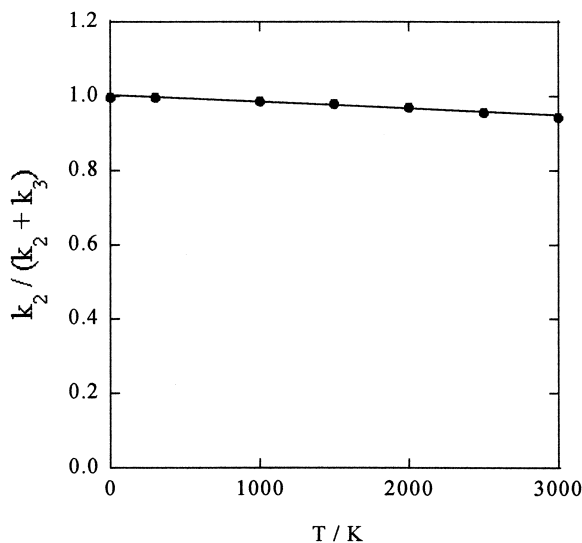


Fig. 17. Calculated temperature dependence of branching ratios for reactions.



is the sum of states at the activated complex with energies of between 0 to E^* . Similarly, $G(E^+)$ is the density of states at the transition state with excess energy, E^+ . Since both reactions (2) and (3) go through the same activated complex, CSO₂, the sum of states, $N(E^*)$, is the same for both reactions, and therefore the branching ratios between reactions (2) and (3) are determined by the ratio of the sum of states, $G(E^+)$, at the transition states. Using the Whitten-Rabinovitch approximation³⁷ to calculate the sum of states, $G(E^+)$, the branching ratios for reactions (2) and (3) were obtained. The temperature dependence of the branching ratio is shown in Fig. 17. From these calculations, it was concluded that reaction (2) was the dominant channel for the reaction CS + O₂ below 3000 K, and reaction (3) was found to make negligible contributions to the CS + O₂ reaction, as was proposed by Sheen et al.²¹ In this work, the activation energy for reaction (2) was determined to be about 50 kJ mol⁻¹, but the activation energy of TS1 is much below the total energy of the reactants. The high activation energy for reaction (2) was also inferred by Black et al.⁶ and Richardson et al.,⁷ because the rate constant for reaction (2) was very slow at room temperature. The most probable explanation for such conflicts is that the reaction CS + O₂ → CSO₂ has an activation energy of about 50 kJ mol⁻¹, and this reaction is a rate-controlling process for the reaction of CS + O₂. On the other hand, exit barriers of the transition states TS1 and TS2 only determine the branching ratios for reactions (2) and (3). In this calculations, the transition state for the entrance barrier of CS + O₂ → CSO₂ could not be determined. Further work is necessary for more accurate predictions of these rate

constants and a comparison with the experimental results.

Conclusion

In the present work we measured the kinetic behavior of S and O atoms, which were the important products of the CS₂ combustion process at high temperature. To explain the temporal behavior of these atomic species, the rate constants for both reactions, CS + O → CO + S and CS + O₂ → COS + O, were determined. The oxidation mechanism of COS has also been carried out, and the rate constant for the reactions COS + Ar → CO + S + Ar and S + O₂ → SO + O were determined.

References

- 1 F. R. Taylor and A. L. Myerson, Proc. 7th Symposium (International) on Combustion, The Combustion Institute, 1959, p. 72.
- 2 A. L. Myerson and F. R. Taylor, *J. Am. Chem. Soc.*, **75**, 4348 (1953).
- 3 W. P. Wood and J. Heicklen, *J. Phys. Chem.*, **75**, 861 (1971).
- 4 F. J. Wright, *J. Phys. Chem.*, **64**, 1648 (1960).
- 5 M. Sargo, A. Yarwood, O. Strausz, and H. Gunning, *Can. J. Chem.*, **43**, 1886 (1965).
- 6 G. Black, L. E. Jusinski, and T. G. Slanger, *Chem. Phys. Lett.*, **102**, 64 (1983).
- 7 R. J. Richardson, *J. Phys. Chem.*, **79**, 1153 (1975).
- 8 N. Djeu, *J. Chem. Phys.*, **60**, 4109 (1974).
- 9 G. Hancock, C. Morley, and I. W. Smith, *Chem. Phys. Lett.*, **12**, 193 (1971).
- 10 R. D. Suart, P. H. Dawson, and G. H. Kimell, *J. Appl. Phys.*, **43**, 1022 (1972).
- 11 I. R. Slage, J. R. Gilbert, and D. Gutman, *J. Chem. Phys.*, **61**, 704 (1974).
- 12 G. T. Bida, W. H. Breckenridge, and W. S. Kolln, *J. Chem. Phys.*, **64**, 3296 (1976).
- 13 H. V. Lilenfeld and R. J. Richardson, *J. Chem. Phys.*, **67**, 3991 (1977).
- 14 H. G. Schecker and H. G. Wagner, *Int. J. Chem. Kinet.*, **1**, 541 (1969).
- 15 D. Woiki and P. Roth, *Ber. Bunsen-Ges. Phys. Chem.*, **96**, 1347 (1992).
- 16 M. Oya, H. Shiina, K. Tsuchiya, and H. Matsui, *Bull. Chem. Soc. Jpn.*, **67**, 2311 (1994).
- 17 K. Saito, Y. Ueda, R. Ito, T. Kakumoto, and A. Imamura, *Int. J. Chem. Kinet.*, **18**, 871 (1986).
- 18 A. Miyoshi, H. Shiina, K. Tsuchiya, and H. Matsui, 26th Symposium (International) on Combustion, The Combustion Institute, 1996, p. 535.
- 19 D. Woiki and P. Roth, *Int. J. Chem. Kinet.*, **27**, 59 (1995).
- 20 T. Just, in "Shock Waves in Chemistry," ed by A. Lifshitz, Marcel Dekker Inc, New York and Basel (1981), Chap. 6.
- 21 D. B. Sheen, *J. Chem. Phys.*, **52**, 648 (1970).
- 22 R. J. Kee, F. M. Rupley, and J. A. Miller, CHEMKIN II, A Fortran Chemical Kinetics Package for Analysis of Gas-Phase Chemical Kinetics, Sandia Report SAND89-8009B, 1989.
- 23 R. J. Kee, F. M. Rupley, and J. A. Miller, The Chemkin Thermodynamics Data Base, Sandia Reprint SAND87-8215B, 1987.
- 24 A. G. Gaydon, G. H. Kimbell, and H. B. Palmer, *Proc. R. Soc. London.*, **279**, 313 (1964).
- 25 H. A. Olschowski, J. Troe, and H. G. Wagner, *Ber. Bunsen-Ges. Phys. Chem.*, **70**, 1060 (1966).
- 26 K. Saito, Y. Toriyama, T. Yokubo, T. Higashihara, and I. Murakami, *Bull. Chem. Soc. Jpn.*, **53**, 1437 (1980).
- 27 K. Hatarajan and P. Roth, *Combust. Flame.*, **70**, 267 (1987).
- 28 I. W. M. Smith, *Trans. Faraday Soc.*, **64**, 378 (1968).
- 29 A. A. Westenberg and N. de Haas, *J. Chem. Phys.*, **50**, 5076 (1969).
- 30 K. H. Homann, G. Krome, and H. G. Wagner, *Ber. Bunsen-Ges. Phys. Chem.*, **72**, 998 (1968).
- 31 C. N. Wei and R. B. Timmons, *J. Chem. Phys.*, **62**, 3240 (1975).
- 32 D. W. Howgate and T. A. Barr Jr., *J. Chem. Phys.*, **59**, 2815 (1973).
- 33 M. J. Frisch, G. W. Trucks, M. Head-Gordon, P. M. W. Gill, M. W. Wong, J. B. Foresman, B. G. Johnson, H. B. Schlegel, M. A. Robb, E. S. Replogle, E. S. Gomperts, J. L. Andres, K. Raghavachari, J. S. Binkley, C. Gonzales, R. L. Martin, D. J. Fox, D. J. DeFrees, J. Baker, J. J. P. Stewart, and J. A. Pople, Gaussian 98, Gaussian, Inc, Pittsburg, PA, 1998.
- 34 D. L. Baulch, D. D. Drysdale, J. Duxbury, and S. Grant, "Evaluated Kinetics Data for High Temperature Reactions," Butterworths, London (1972), vol. 3.
- 35 A. Lifshitz, *Int. J. Chem. Kinet.*, **7**, 753 (1975).
- 36 J. Hardy and W. C. Gardiner, Jr., Proc. 16th Symposium (International) on Combustion, The Combustion Institute, 1976, p. 785.
- 37 G. Z. Whitten and B. S. Rabinovitch, *J. Chem. Phys.*, **38**, 2466 (1963).